Asian Journal of Chemistry; Vol. 33, No. 9 (2021), 2219-2228

ASIAN JOURNAL OF CHEMISTRY

https://doi.org/10.14233/ajchem.2021.23386

Corrosion Inhibition of Mild Steel in 0.5 M H_2SO_4 Solution by Plant Extract of *Annona squamosa*

S. KARTHIKEYAN[1], S.S. SYED ABUTHAHIR[1,*], A. SAMSATH BEGUM[1] and K. VIJAYA[2]

[1]Department of Chemistry, Jamal Mohamed College (Autonomous), (Affiliated to Bharathidasan University), Tiruchirappalli-620020, India
[2]Department of Chemistry, PSNA College of Engineering and Technology (Affiliated to Anna University, Chennai), Dindigul-624622, India

*Corresponding author: E-mail: syedchem05@gmail.com

Received: 27 June 2021; *Accepted*: 9 August 2021; *Published online*: 20 August 2021; AJC-20487

In aqueous solution of 0.5 M H_2SO_4, the *Annona squamosa* extract was systematically analyzed to ensure its inhibition mechanism by using potentiodynamics polarization, the weight loss method, and electrochemical impedance spectroscopy (EIS) and its inhibitory effect on mild steel corrosion. For mild steel corrosion in 0.5 M H_2SO_4 solution, its inhibition efficiency increases and decreases with an increase in its concentration and temperature, respectively. Potentiodynamic polarization analyses revealed that the *Annona squamosa* behaves as a cathodic inhibitor. In presence of *Annona squamosa* extract in 0.5 M H_2SO_4 solution, an increase in the activation energy of corrosion leads to a decrease in the rate of mild steel corrosion. On mild steel surfaces, the adsorption behaviour of the extract conformed to the Temkin isotherm, Langmuir isotherm and Arrhenius equation. The EIS results were correlated with the polarization findings. According to atomic force microscopy (AFM) and scanning electron microscopy (SEM), the inhibition of mild steel corrosion proceeds through the adsorption of the extract on the mild steel surface.

Keywords: *Annona squamosa*, Acid corrosion, Acid inhibition.

INTRODUCTION

Since the industrial revolution for industrial and structural applications, mild steel is the most commonly employed alloy. In the investigation of mild steel corrosion, the use of acidic media is crucial due to its industrial applications, including industrial cleaning, acid pickling, acid descaling, petrochemical processes and oil-well acid in oil recovery [1-3]. Crude oil is refined under various corrosive conditions and equipment corrosion usually results from a strong acid that attacks the surface of the equipment. In numerous industrial and structural applications of mild steel, the equipment is exposed to a corrosive environment, and it is susceptible to various corrosion processes. Thus, to avoid metal dissolution, the use of corrosion inhibitors is inevitable. Inhibitor utilization is a highly practical method for corrosion protection, specifically in the acidic media. Most of the well-known inhibitors include organic compounds having multiple bonds and hetero atoms, including N, O, and S. Among these organic compounds, most of them are expensive and toxic to both the environment and humans. Therefore, researches have put efforts to develop non-toxic and cost-effective corrosion inhibitors.

Plant extracts are regarded as an abundant source of the environmental friendly corrosion inhibitors. Several leaves, flowers, roots and seeds extracts were tested successfully as corrosion inhibitors such as *Schinopsis lorentzii* [4], *Tabernaemontana* divaricate [5], almond fruit [6], *Thymus algeriensis* [7], *Musa acuminate* [8], *Euphorbia falcata* [9], *Tagetes erecta* [10], *Osmanthus fragran* [11], *Nerium oleander* [12], orange fruit [13] and *Ferula harmonis* [14]. In literature, many plant extracts have been used as corrosion inhibitor for mild steel in different acidic media such as *Ligularia fischeri* extract [15], *Glycyrrhiza glabra* leaves extract [13], *Ziziphora* leaves extract [16], nettle extract [17], primrose flower extract [18], *Rosa damascene* flower extract [19], mustard seed extract [20], *Urtica dioica* leaves extract [20], *Eucalyptus* leaves extract [21], litchi fruit extract [22] were applied for mild steel in HCl medium. The plant possesses several classes of phytoconstituents. The main classes are terpenoids, terpene derivatives, flavonoids, alkaloids, glycoside, diazepine, squamolone and 11-hydroxy-16-hentriacontanone. Some researchers [23] has isolated twelve compounds from *Annona Squamosa* and their structures were identified as liriodenine, moupinamide-(-)-kauran-16α-ol-19-oic acid, 16β,17-dihydroxy-(-)-kauran-

19-oic acid, anonaine, 16α,17-dihydroxy-(-)-kauran-19-oic acid, (-)-isokaur-15(16)-en-17,19-dioic acid, squamosamide, 16α-methoxy-(-)-kauran-19-oic acid, sachanoic acid, (-)-kauran-19-al-17-oic acid, daucosterol, *etc*.

The main aim of the present study is to assess the inhibitive influence of *Annona squamosa*l leaves extract on the mild steel corrosion in 0.5 M H_2SO_4 using weight loss and electrochemical techniques [open circuit potential (OCP), potentiodynamic polarization and electrochemical impedance spectroscopy (EIS)]. The achieved results will be confirmed by surface morphology analysis of the surface layer of the mild steel specimens using FTIR, SEM and AFM techniques.

EXPERIMENTAL

Mild steel specimens (27.36% O, 8.23% C and the rest iron) of dimensions 1.0 cm × 4.0 cm × 0.2 cm were polished to mirrors finish and degreased with acetone and used for weight loss method. A solution of 0.5 M H_2SO_4 was prepared using double distilled water.

Preparation of inhibitor: Double distilled water and analytical reagents grade chemicals (E. Merk, India, AR Grade) were used for preparing solutions. *Annona squamosa* was dried for 6 h in an oven at 70 ºC and grinded. About 10 g of *Annona squamosa* powder was refluxed in100 mL double distilled water for 1 h. The extract of the plant was prepared by evaporating the filtrate. The required concentrations of solution were prepared by using the residues in aqueous solution of 0.5 M H_2SO_4.

Phytoconstituents of *Annona squamosa*: Extensive phytochemical evaluations on different portions of *A. squamosa* plant have shown the presence of various phytochemicals and constituents including diterpenes and alkaloids. The main classes are terpenoids, flavonoids, glycoside, diazepine, squamolone and 11-hydroxy-16-hentriacontanone. Six major components were identified as 1*H*-cycloprop(e)azulene (3.46%), germacrene D (11.44%), bisabolene (4.48%), caryophyllene oxide (29.38%), bisabolene epoxide (3.64%) and kaur-16-ene (19.13%) [24]. Detection of three new compounds *viz*. *Annonaceous acetogenins*, (2,4-*cis* and *trans*)-squamolinone, (2,4-*cis* and *trans*)-9-oxoasimicinone and bullacin B was also reported in the literature [25,26].

Weight loss method: In this study, the experiments were carried out by varying the concentrations of the inhibitor. The study was also carried out at different temperatures and the immersion period was fixed at 3 h. The results obtained were discussed to know the effect of concentration:

$$IE\ (\%) = [1 - (W_2 - W_1)] \times 100 \quad (1)$$

where W_1 is the weight loss in the absence of inhibitor and W_2 is weight loss in the presence of inhibitor and temperature [27]. The corrosion rate decreases and the inhibition efficiency increases with increase in concentration of extract for all inhibitors, while the concentration range was 2% to 10% for 3 h immersion of the metal coupon in corrodent solution at room temperature.

The inhibition efficiency increases due to the inhibitor molecules present in plant extract getting adsorbed on the mild steel surface [28]. The maximum inhibition efficiency and the lower corrosion rate is found at high concentration 10% v/v for all inhibitors. With further increase in inhibitor concentration above 10%, the inhibition efficiency and corrosion rate almost remained constant. So 10% concentration was fixed as the concentration for maximum inhibition for inhibitor. This concentration corresponds to the attainment of a saturation value in surface coverage of metal [29]. The comparison of performance of inhibitors show that the maximum efficiency and low corrosion rate was found for *Annona squamosa* system.

Effect of temperature: Temperature effect would be high on mild steel corrosion in acid medium. Inhibitor efficiency depends on temperature was used to determine activation energy (E_a) of corrosion of the mild steel in the presence and in the absence of the inhibitors. It was used to identify the mechanism of the action of inhibitor on mild steel corrosion. The temperature factor is most important parameter in corrosion studies and also the effect of the temperature on the inhibitive nature is examined by weight loss method. The study of temperature effect on corrosion at different concentrations of the inhibitor in the different temperatures *viz*. 303, 313, 323 and 333 K for the immersion period of 3 h have been adopted.

Adsorption isotherms: Phytoconstituents present in the extracts are possibly adsorbed on the mild steel surface and the degree of adsorption depends on, temperature and the electrochemical potential at the metal solution interface [30]. The degree of surface coverage (θ) with respect to different concentrations of the inhibitor and different temperatures have been determined to deduce the fittest isotherm. In this work, adsorption parameters obtained from Langmuir and Tempkin adsorption isotherms for the corrosion inhibitive effect of aqueous leaf extracts of *Annona squamosa* on the corrosion of mild steel in 0.5 M H_2SO_4.

Electrochemical methods: Potentiodynamic polarization and electrochemical impedance were measured with electrochemistry software by using the CHI6608 Microcell kit Princeton electrochemical analyser of PC-controlled electrochemical impedance analyzer model. These analyses were performed in a typical three-cell electrode with the total volume of 100 mL. The employed counter and reference electrodes were the cylindrical graphite and saturated calomel electrodes, respectively. The working electrode of mild steel was abraded with various grade emery sheets. Then, it was washed before each run. The working electrode area was 3.14 cm^2 and this electrode was immersed into inhibited and uninhibited acidic solutions for OCP tests. In both the cathodic and anodic directions, potential changes began from OCP (E_{ocp}) during polarization measurements. The potential scan rate was set to 0.17 mV s^{-1}. The working electrode was immersed in the analyzed solution for 0.5 h to obtain sufficient time for E_{ocp} to stabilize.

FT-IR analysis: Perkin Elmer FT-IR spectrophotometer was used to record the FT-IR spectrum from 4000 to 400 cm^{-1}. The adsorbed plant leaf extract inhibitor on metal surface have been analyzed by FT-IR spectra [31]. After, it was scratched from the mild steel surface, which was immersed in 0.5 M H_2SO_4 in presence of plant leaf extract inhibitors for 3 h at room temperature.

UV-visible analysis: To prove metal-inhibitor complex formation on the mild steel surface, a double beam spectrophotometer based on PC was employed. UV-visible absorption spectrophotometry was performed to analyze a solution comprising mild steel, which was immersed in 0.5 M H_2SO_4 with 10% (v/v) *Annona squamosa* extracts for 3 h at room temperature and the crude plant extract [32].

Scanning electron microscope (SEM): The difference in the nature of metal surface before and after the mild steel surface with the corrodent solution was examined in order to observe the effect of the addition of inhibitor [33]. Thus, SEM was used to analyze the topography of mild steel surface after corroding in presence and absence of the inhibitor. The SEM image was taken by the SEM instrument, JEOL MODEL JSM 6390.

Atomic force microscopy (AFM): Surface morphology was also characterized by using an atomic force microscopy. After the inhibition test, the mild steel specimens were placed in vacuum desiccators, mounted on sample holder under the objective of the atomic force microscope and the 3D-images were taken from the 100 × magnified surface through operating program on computer. The surface of mild steel specimens after immersed in 0.5 M H_2SO_4 solution in the absence and presence of aqueous leaf extract of *Annona squamosa*, for 2 h were evaluated by atomic force microscopy analysis [34]. From the AFM cross sectional 3D-image, the line and surface roughness parameters of the specimens such as R_a, R_q and peak to valley value were obtained for the mild steel after immersion in 0.5 M H_2SO_4 in the absence and presence of the inhibitor.

RESULTS AND DISCUSSION

The corrosion rates (CR) of mild steel immersed in 0.5 M H_2SO_4 and also inhibition efficiencies (IE) in the absence and presence of the extract of the extract of *Annona squamosa* inhibitor obtained by weight loss method are given in Table-1. It is observed that 10% *Annona squamosa* extract offers 97.8 % of inhibition efficiency in an aqueous solution of 0.5 M H_2SO_4. It is observed (Table-1) that the *Annona squamosa* extract shows a good inhibition efficiency. As the concentration of the extract of *Annona squamosa* increases, the IE increases, which is due to an increase of surface coverage at higher concentration of *Annona squamosa* that retards dissolution of mild steel. The possibility of interaction between the hetero atoms present in the plant leaf extract and metal ions from the metal surface can be attributed for higher inhibition efficiencies. The presence of many phytochemical constituents in the plant extracts are responsible for the inhibition of mild steel corrosion and this can be attributed the reasons for the anticorrosive actions of plant extracts. This observation is in good agreement with the reported results [35,36].

TABLE-1
INHIBITION EFFICIENCY OF AQUEOUS LEAVES EXTRACT OF *Annona squamosa* ON THE CORROSION OF MILD STEEL IN 0.5 M H_2SO_4 AT ROOM TEMPERATURE (303 K)

Concentration of inhibitor (%)	Corrosion rate (mmd)	Inhibition efficiency (%)
Blank	328.13	–
2	164.10	50.0
4	71.333	78.3
6	53.50	83.7
8	28.53	91.3
10	7.133	97.8

Adsorption isotherm: An adsorption isotherm gives the direct relationship between the corrosion inhibition efficiency with the degree of surface coverage at constant temperature for different concentrations of inhibitor solutions. The adsorption isotherm provide the basic information about the nature of interaction between the mild steel surface and inhibitor molecular constituents [37].

Temkin adsorption isotherm: Temkin adsorption isotherm is based on the assumption of the uniform distribution of the inhibitor (monolayer) on the mild steel surface. The adsorption energy linearly decreases with the increase of surface coverage values (θ). The values of surface coverage θ at various concentrations of each inhibitor in 0.5 M H_2SO_4 solution, obtained from mass loss measurements, were fitted to Temkin adsorption isotherm as shown below:

$$\exp(-2a\theta) = K_{ads} \cdot C$$

$$\theta = -2.303 \log K_{ads}/2a - 2.303 \log C/2a$$

where, a denotes the lateral molecular interaction parameter. The adsorption of organic molecules at a metal-solution interface is a quasi-substitutional process between the inhibitor molecule (in aqueous solution) and water molecule (on the mild steel surface) [38].

Adsorption parameters obtained from Langmuir and tempkin adsorption isotherms for the corrosion inhibitive effect of aqueous leaf extracts of *Annona Squamosa* on the corrosion of mild steel in 0.5 H_2SO_4 are given in Tables 2 and 3.

Activation energy (E_a): The energy of activation for the corrosion of mild steel in 0.5 M H_2SO_4 was determined using the Arrhenius type of plot using the following equation [39]:

$$\log CR = K \exp\left(-\frac{E_a}{RT}\right)$$

where, CR = corrosion rate, R = universal gas constant, E_a = energy of activation, T = absolute temperature and K = Arrhenius pre-exponential constant. The values of E_a is calculated for mild steel in the presence and in the absence of all studied

TABLE-2
ADSORPTION PARAMETERS OBTAINED FROM LANGMUIR ADSORPTION ISOTHERM FOR THE CORROSION INHIBITIVE EFFECT OF AQUEOUS LEAF EXTRACTS OF *Annona squamosa* ON THE CORROSION OF MILD STEEL IN 0.5 H_2SO_4

Inhibitor system	Temperature (K)	R^2	Slope	Intercept	K_{ads}	$-\Delta G°_{ads}$ (KJ mol^{-1})
Annona squamosa	303	0.992	0.805	2.230	0.4484	8.100
	313	0.991	0.930	2.220	0.4500	8.400
	323	0.992	1.000	2.500	0.4000	8.330
	333	0.994	0.995	3.170	0.3150	7.930

TABLE-3
ADSORPTION PARAMETERS OBTAINED FROM TEMKIN ADSORPTION ISOTHERM FOR THE CORROSION INHIBITIVE EFFECT OF AQUEOUS LEAF EXTRACTS OF *Annona squamosa* ON THE CORROSION OF MILD STEEL IN 0.5 M H_2SO_4

Inhibitor system	Temperature (K)	R^2	Slope	Intercept	-a	K_{ads}	$-\Delta G°_{ads}$ (KJ mol^{-1})
Annona squamosa	303	0.9686	0.6577	0.3307	1.750	3.1800	13.034
	313	0.9507	0.5637	0.3217	2.040	3.7147	13.870
	323	0.9632	0.5502	0.2796	2.093	3.2230	13.930
	333	0.9786	0.5481	0.2237	2.100	2.5580	13.722

inhibitor *Annona squamosa* from the slope value of log CR *vs.* 1/T plots (figures not shown) and the E_a values are shown in Table-4.

TABLE-4
AVERAGE ACTIVATION ENERGY FOR CORROSION OF MILD STEEL IN 0.5 M H_2SO_4 IN THE ABSENCE AND IN THE PRESENCE OF *Annona squamosa* LEAF AQUEOUS EXTRACT (10% v/v)

Inhibitor system	E_a (KJ/mol)
Blank	19.2
ASLE	84.2

Electrochemical analysis: The electrochemical measurements extend a way for calculating the rate of corrosion of a mild steel. It permits quick evaluation of the performance of inhibitor, durability of surface film and also the rate of corrosion. In this study, the electrochemical techniques (*viz.* potentiodynamic polarization and electrochemical impedance spectroscopy) were used for mild steel corrosion in 0.5 M H_2SO_4 in absence and in presence of the studied inhibitor, *Annona squamosa* to know whether they are cathodic or anodic or mixed type inhibitor and also to formulate an appropriate mechanism for their inhibition action on corrosion.

Potentiodynamic polarization: Polarization study has been used to confirm the formation of protective film on the mild steel surface during corrosion inhibition process. If a protective film is formed on the mild steel surface, the linear polarization resistance values (LPR) increases and the corrosion current value (I_{corr}) decreases and corrosion potential increases (E_{corr}) [40]. The potentiodynamic polarization curves of mild steel immersed in an aqueous solution 0.5 M H_2SO_4 and in absence and presence of *Annona squamosa* are shown in Fig. 1. The corrosion parameters are given in Table-5. When mild steel was immersed in an aqueous solution of 0.5 M H_2SO_4 the corrosion potential was -0.468 mV *vs.* SCE. When *Annona squamosa* 10% was added to the above system, the corrosion potential shifted to the cathodic side -0.465 mV *vs.* SCE. This indicates that the protective film is formed on the cathodic sites of the mild steel surface. This film controls the anodic reaction of mild steel dissolution by forming complex on the cathodic sites of the mild steel surface. Further, the LPR value

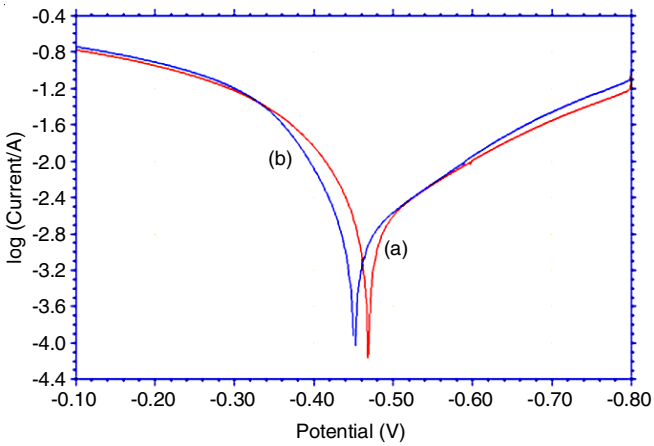

Fig. 1. Potentiodynamic polarization curves for corrosion of mild steel in 0.5 M H_2SO_4; (a) Without inhibitor; (b) With 10% aqueous leaf extract of *Annona squamosa*

in an aqueous solution of 0.5 M H_2SO_4 increases from 9.5 ohm cm^2 to 16.9 ohm cm^2, the corrosion current decreases from 3.459×10^{-3} A/cm^2 to 1.950×10^{-3} A/cm^2. Thus polarization study confirms the formation of a protective film on the mild steel surface.

Electrochemical impedance spectroscopy: Electrochemical impedance (AC impedance) spectra were used to prove protective film formation on the surface of mild steel. When the protective film was produced on the surface of mild steel, the charge transfer resistance (R_t), impedance log (Z/ohm) and double layer capacitance (C_{dl}) increased, increased and decreased, respectively [41]. The Bode and Nyquist plots of the electrochemical impedance of mild steel, which was immersed in 0.5 M H_2SO_4 solution in absence and presence of *A. squamosa* are shown in Figs. 2 and 3, respectively. Table-6 presents the AC impedance parameters, such as double-layer capacitance (C_{dl}) and charge-transfer resistance (R_t), which were derived using the Nyquist plots. Table-6 also presents the values of impedance log (Z/ohm), which were obtained using the Bode plots. In 0.5 M H_2SO_4 medium, when *A. Squamosa* inhibitor was added, the R_t and C_{dl} values exhibited an increase and a decrease, respectively, from 13.88 to 56.993 Ω cm^2 and from 2.108026×10^{-6} to 8.650830×10^{-6} F cm^2, respectively.

TABLE-5
CORROSION PARAMETERS OF MILD STEEL IN AN AQUEOUS SOLUTION OF 0.5 M H_2SO_4 AND IN THE ABSENCE AND PRESENCE *Annona squamosa* SYSTEM OBTAINED BY POTENTIODYNAMIC POLARIZATION METHOD

Concentration of the aqueous leaf of AS (%V/V)	$-E_{corr}$ (Mv/SCE)	Tafel slope		I_{corr} (A/cm^2)	LPR (Ω/cm^2)
		ba (mV/dec)	bc (mV/dec)		
0	-0.468	7.893	5.397	3.459×10^{-3}	9.5
10	-0.465	5.480	7.722	1.950×10^{-3}	16.9

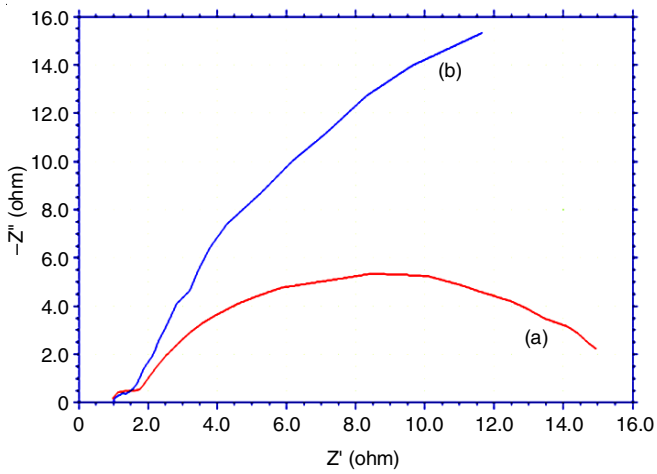

Fig. 2. Nyquist plot for the corrosion of (a) Mild steel in 0.5 M H_2SO_4 without inhibitor, (b) With 10% aqueous leaf extract of ASLE

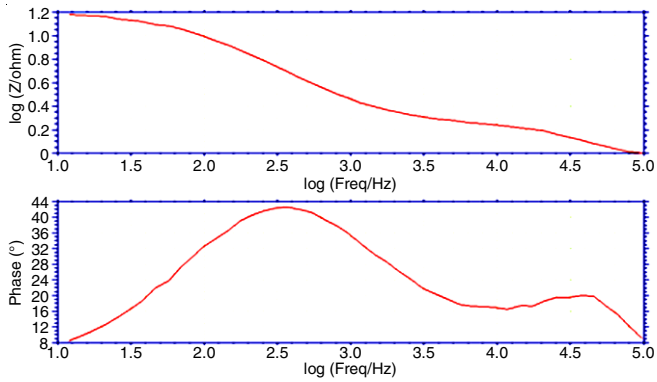

Fig. 3a. Bode plots for the corrosion of mild steel in 0.5 M H_2SO_4 without inhibitor

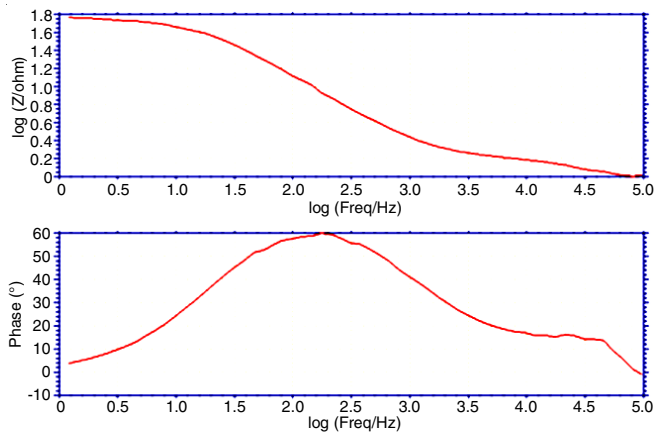

Fig. 3b. Bode plots for the corrosion of mild steel in 0.5 M H_2SO_4 with 10% *Annona squamosa* inhibitor

TABLE-6
ELECTROCHEMICAL IMPEDENCE PARAMETERS FROM NYQUIST PLOTS FOR THE CORROSION OF MILD STEEL WITHOUT AND WITH THE VARIOUS CONCENTRATIONS OF *Annona squamosa* LEAF AQUEOUS EXTRACT IN 0.5 M H_2SO_4

Concentration of the aqueous leaf extract of AS (%v/v)	Nyquist plot		Impedance log (z/ohm)
	R_{ct} (Ω/cm^2)	C_{dl} (μF/cm^2)	
Blank	13.880	2.108026×10^{-6}	1.17248
10	56.993	8.650830×10^{-6}	1.75104

Further, the [log (Z/ohm)] value increased from 1.17248 to 1.75104. These results indicated the formation of the protective film on the surface of mild steel.

UV-visible spectral analysis: The extracts prepared from a plant leaves have many constituents are responsible for the inhibition of metal corrosion. The constituent chemical compounds, present in the extract, are expected to form complex with the surface of metal during the process of inhibition. The complexes produced are revealed by the UV-visible spectrum analysis. During corrosion in 0.5 M H_2SO_4 acid solution, metal cation is expected to be formed from the surface of the metal and form complexes with inhibitors [42]. The changes in the positions of absorption maxima and the absorbance values revealed the complex formation between the metal surface ions and inhibitor [43]. The pattern of the UV-visible absorption spectra are recorded for the crude extract of plant leaves and the solution of the mixture of mild steel/0.5 M H_2SO_4/10% inhibitor concentrations after 3 h duration (Fig. 4). The absorption bands of corresponding system are enlisted (Table-7).

TABLE-7
UV-VISIBLE SPECTRAL ABSORPTION BANDS OF AQUEOUS *Annona squamosa* AND THE SCRATCHED FILM FROM MILD STEEL AFTER IMMERSION IN 0.5 M H_2SO_4 WITH 10% INHIBITORS

Inhibitor system	Absorption bands (nm)	
	Absorption bands (nm)	Scratched film from mild steel surface
ASLE	269.95	230.45

The UV-visible spectral pattern exhibit the possibility of interaction between the hetero atoms present in the plant leaf extract and metal ion from the metal surface. The UV-visible spectra show that the bands in the region 200 to 350 nm are due to the carbonyl groups held close to Fe^{3+} in the complex forms [43], which might be the reasons for the anticorrosive actions of plant extracts.

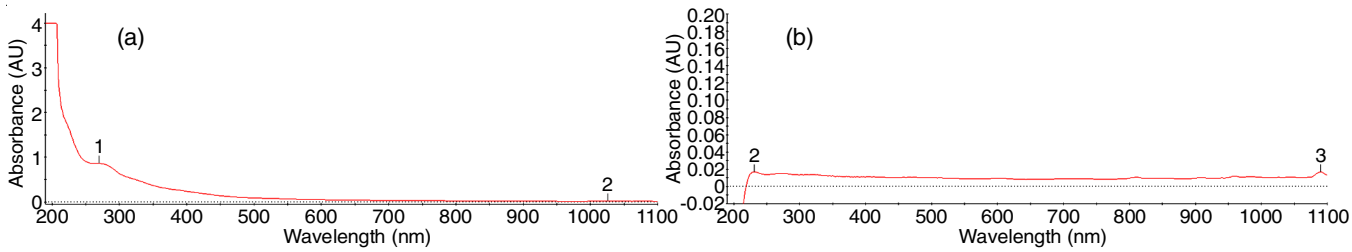

Fig. 4. UV-visible spectra of (a) aqueous leaves extract of *Annona squamosa*; (b) UV-visible spectra of the scratched film from mild steel after immersion in 0.5 M H_2SO_4 with 10% ASLE inhibitor

FT-IR spectral characterization: FT-IR analysis helps to identify the absorption bands for the functional groups and the alignment of inhibitor molecules on the metal surface. The FT-IR spectrum of *A. squamosa* (Fig. 5a) and the FT-IR spectral pattern of the adsorbed layer (Fig. 5b), scratched from the surface of mild steel after immersion in 0.5M H_2SO_4 for 3 h in the presence of higher (10% v/v) concentration of the inhibitor (ASLE) at room temperature have been compared. The absorption bands of the functional groups present in corresponding systems are listed in Table-8.

TABLE-8
FT-IR SPECTRAL DATA FOR THE AQUEOUS LEAVES EXTRACT OF *Annona squamosa* AND THE SCRATCHED FILM FROM MILD STEEL SURFACE AFTER IMMERSION IN 0.5 M H_2SO_4 WITH 10% *Annona squamosa*

IR bands of crude AS plant extract	IR bands of film from mild steel surface	Frequency assignment to functional groups
3435.82	3435.71	-OH
2077.79	2925.08	C-H
1633.89	1632.23	C=C
–	1383.95	O-H bending
1032.67	1120.84	C-O
1014.94	–	C-H Stretch
680.0	–	N-H
–	620.48	CH "oop"
–	473.78	Y-Fe_2O_3

The FT-IR spectrum of *A. squamosa* shows a broad peak at 3435.82 cm^{-1} is attributed to O-H group [44]. The frequency at 2077.79 cm^{-1} correspond to the aliphatic C-H stretching frequencies and the peak at 1633.89 cm^{-1} has been assigned to C=C. The noticeable band at 1032.67 cm^{-1} can be attributed to C-O frequency. The peak present at 1014.94 cm^{-1} has been assigned to C-H stretching frequency. The presence of N-H is identified at 680 cm^{-1}.

The scratched film shows a shift of the O-H stretching from 3435.82 to 3345.71 cm^{-1} indicates that molecular adsorption possibly occurs *via* O-H [45]. The shift in frequency from 2077.79 to 2925.08 cm^{-1} are noticed for C=H group. The shift in frequency from 1633.89 to 1632.23 cm^{-1} are attributed to C=C group. The peaks at 1383.95 cm^{-1} are ascribed for O-H bending group and the peaks at 1355.12 cm^{-1} are observed for C-N group. The shift from 1014.94 to 1120.84 cm^{-1} is noticed for C-O group, while the peak at 620.48 are attributed to CH "oop". The band 473.78 cm^{-1} considerably originate mainly from Fe-complex [46] steel in acid medium.

SEM studies: In present evaluation, the SEM micrograph of the polished mild steel specimen index in the protected condition has been recorded and is presented in Fig. 6a. In the SEM images, surface of the mild steel specimens is smooth and no corrosion product on the surface of the metal was observed.

The SEM micrograph of the mild steel specimen after the immersion in 0.5 M H_2SO_4 for 3 h at room temperature, the image is shown in Fig. 6b. It reveals the complete destruction or deterioration of the smoothness of the metal surface and formation of corrosion spots on it. The image shows that due to the corrosion, the metal surface is highly damaged. The SEM micrographs of the mild steel specimen after immersion period for 3 h at room temperature in 0.5M H_2SO_4 solution in presence of inhibitor *Annona squamosa* leaf extracts at higher concentration (10%) are shown in Fig. 6c. It is suggested that the inhibitor was absorbed into the mild steel to produce a protective layer to prevent the corrosion process on the surface [47].

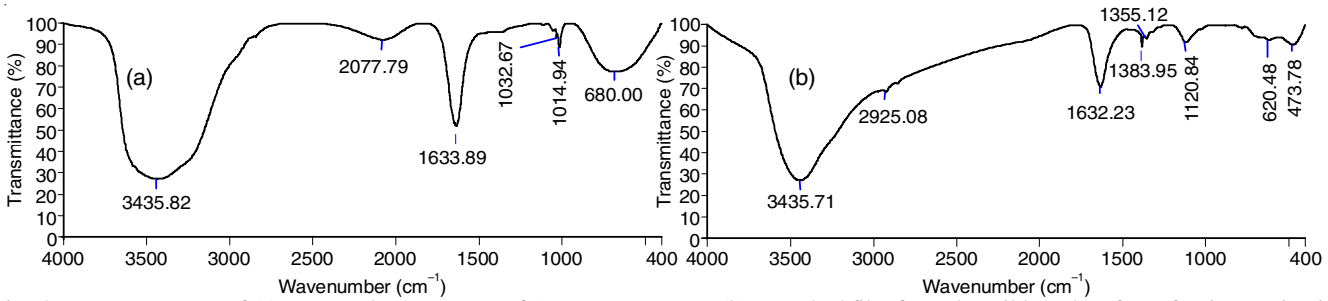

Fig. 5. FT-IR spectrum of (a) aqueous leaves extract of *Annona squamosa*; (b) scratched film from the mild steel surface after immersion in 0.5 M H_2SO_4 with 10% aqueous leaf extract of *Annona squamosa*

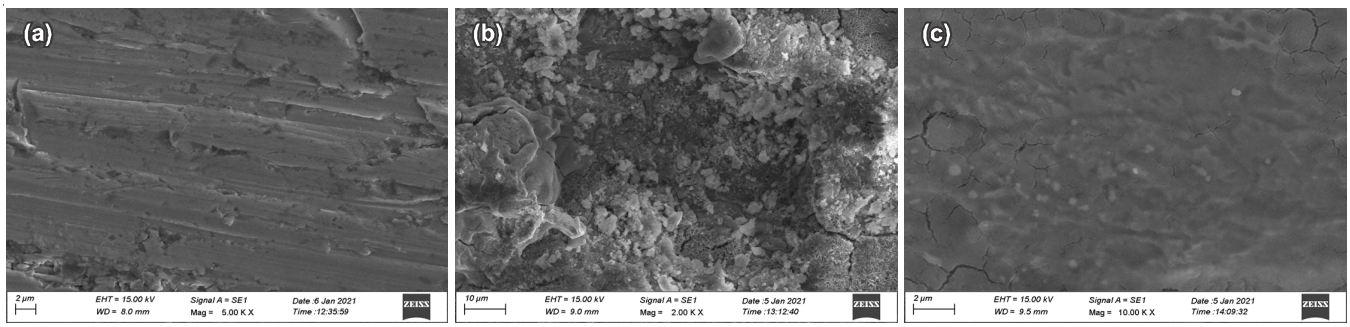

Fig. 6. SEM image of (a) polished mild steel coupon before immersion in 0.5 M H_2SO_4; (b) mild steel coupon after immersion in 0.5 M H_2SO_4; (c) polished mild steel coupon after immersion in 0.5 M H_2SO_4 in the presence of 10% aqueous leaves extract of *Annona squamosa*

Atomic force microscopy (AFM): The useful parameters observed from the 3D images of AFM analysis, are average roughness (R_a), root mean square roughness (R_q) and peak-to-valley value are noted. Among all the parameters, the average roughness (R_a) calculated from the average deviation of roughness, for all points from a mean line over the evaluation length, plays an important role in giving an idea about the nature of the protective adsorbed layer on the mild steel surface. The 3D AFM morphologies and the AFM cross sectional profiles of polished mild steel and mild steel after immersion in 0.5 M H_2SO_4 for 3 h at room temperature are shown in Fig. 7. The AFM cross sectional images of the mild steel coupon after being immersed for 3 h at room temperature in 0.5 M H_2SO_4 in the presence of the high concentrations of leaves extract of *Annona squamosa* are shown in Fig. 7c.

The different parameters R_q, R_a and R_y from the AFM images of metal surfaces are given in Table-9 for the polished mild steel and that after immersion in the absence and presence 10% of the inhibitor *Annona squamosa*. The values indicates that the average roughness (R_a) parameter is reached very high for the blank. The small average roughness (R_a) is observed for the polished mild steel. It is found that the R_a values, after the mild steel is immersed in 0.5M H_2SO_4 in presence of the inhibitor at high concentration, is in between the blank and polished mild steel. It is lower than that of the blank and higher than that of the polished metal surface and can be inferred that a protective film is formed on the metal surface [48].

The root mean square roughness (R_q) is the average of the measured height deviations measured from the mean line [49]. For the blank system (Fig. 7a), a few pits in the corroded metal surface is observed and the slight roughness is observed on the polished steel surface (Fig. 7b). It indicates that the roughness is greater in blank steel coupon compared to the polished metal surface. The measured R_q values of the all inhibitor systems *Annona squamosa* are lower than that of blank and higher than that of polished system. The decrease in the R_q and R_a values reflects that the inhibitor molecules from the plant leaf extract, are adsorbed on the mild steel surface, reducing the rate of corrosion and thereby increasing the efficiency of inhibition.

TABLE-9
AFM SURFACE AND LINE ROUGHNESS DATA FOR DIFFERENT SYSTEMS

System	Surface roughness			Line roughness		
	Average roughness (R_a) (nm)	Root mean square roughness (R_q) (nm)	Maximum peak to valley (P-V) height (nm)	Average roughness (R_a) (nm)	Root mean square roughness (R_q) (nm)	Maximum peak to valley (P-V) height (nm)
Polished mild steel	180.64	222.09	1558.8	178.81	219.84	861.06
Mild steel + 0.5 M H_2SO_4	343.05	423.88	2763.4	202.62	249.97	1114.8
Mild steel + 0.5 M H_2SO_4 with 10 % of ASPLE	130.84	171.22	1641.4	134.53	176.29	763.01

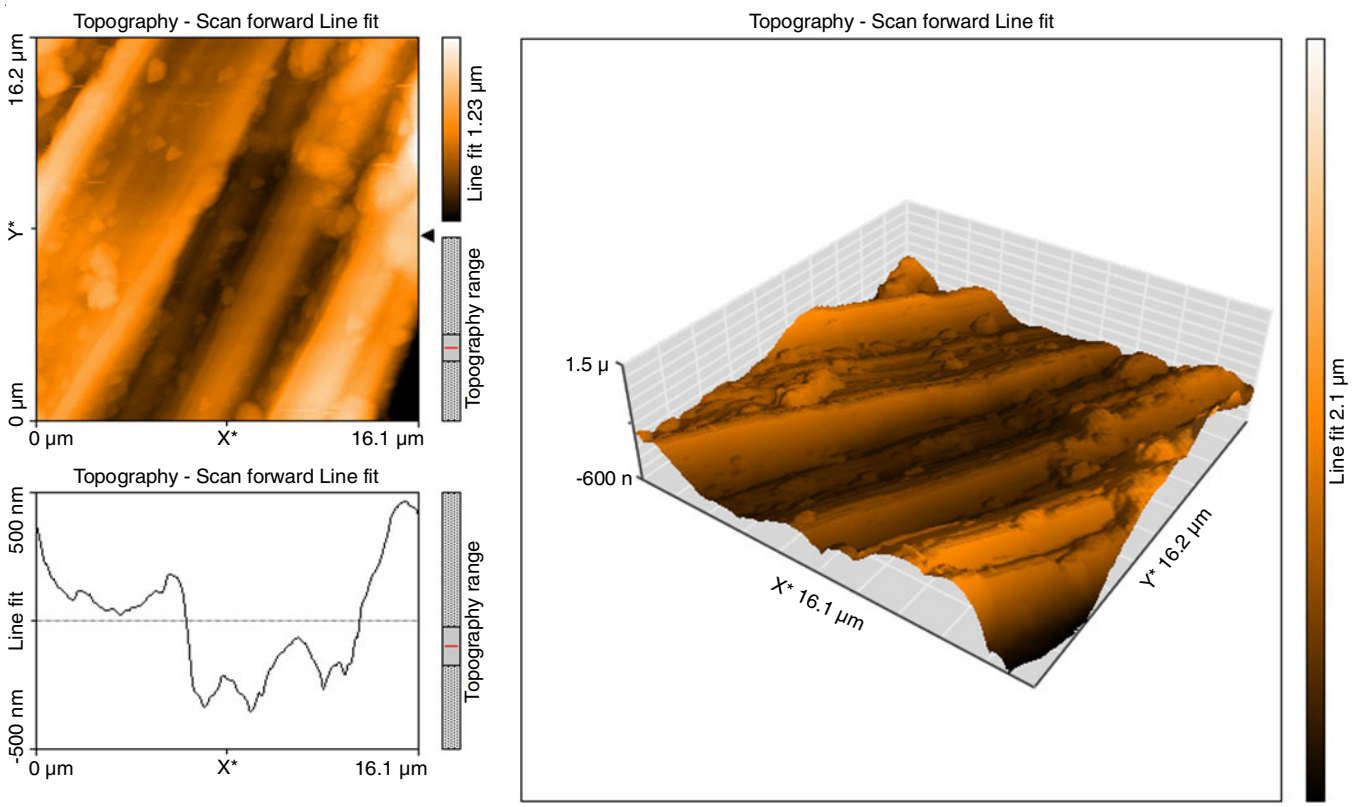

Fig. 7a. AFM cross sectional images of the polished mild steel surface

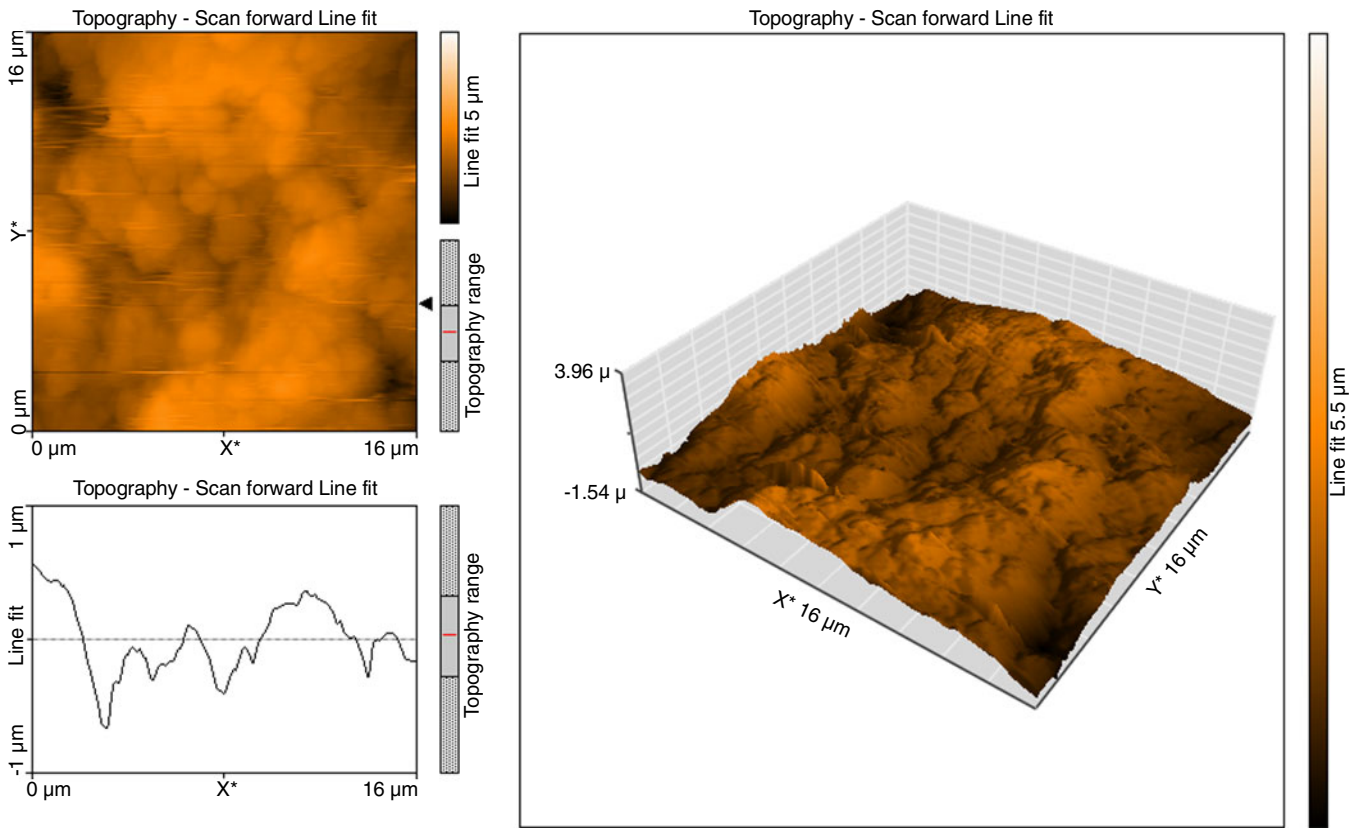

Fig. 7b. AFM cross sectional images of the mild steel surface after immersion in 0.5M H_2SO_4

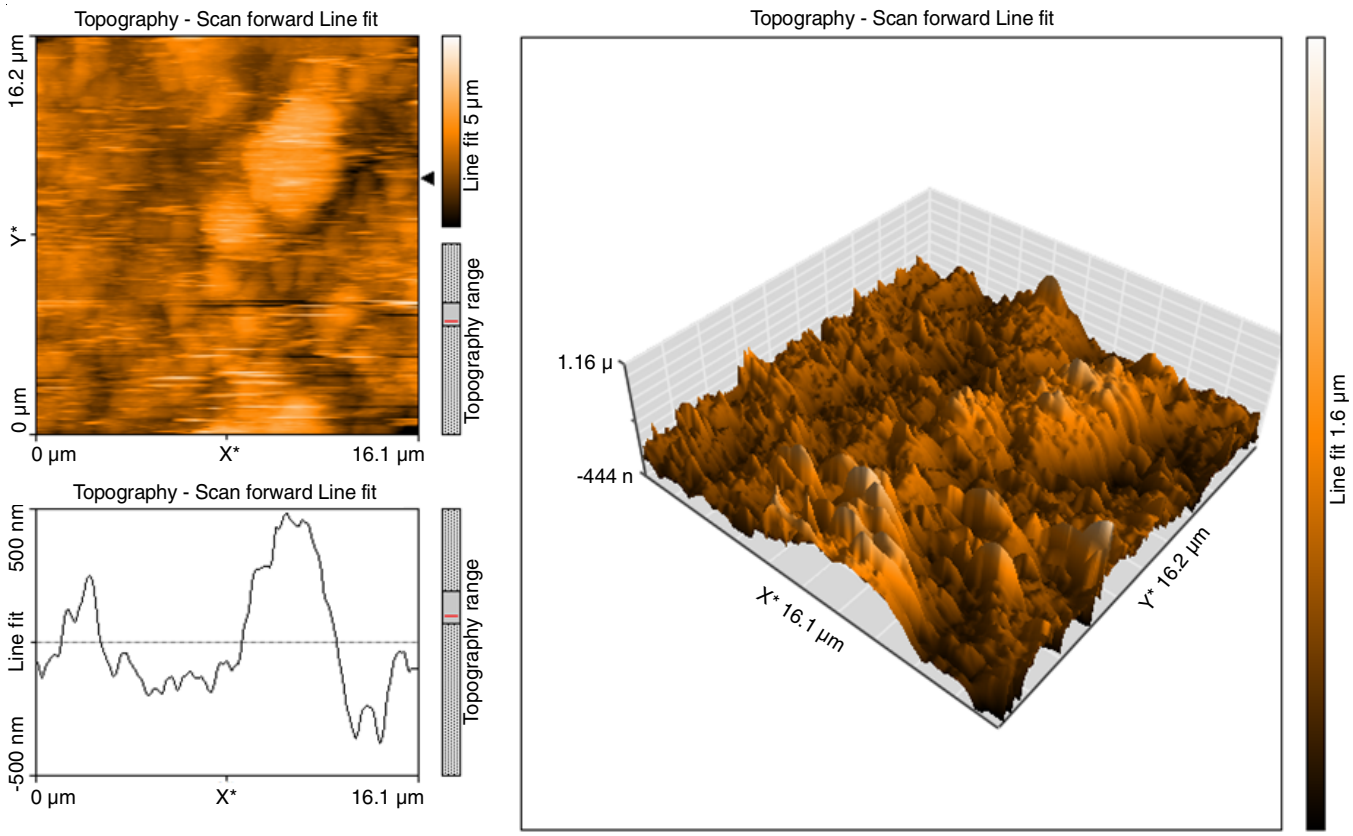

Fig. 7c. AFM cross sectional image for the mild steel surface after immersion in 0.5M $H_2SO_4$with 10% aqueous leaf extract of *Annona squamosa*

The values of the maximum peak-to-valley hight (P-V) is actually a largest single-peak-to-valley height in five adjoining sampling heights. The (P-V) height for the mild steel surface corroded in 0.5 M H_2SO_4 is greater than that for the polished mild steel. The surface topography of the metal surfaces, in the presence of high concentrations of inhibitor, show that the (P-V) height is greater for the inhibited system compared to the polished system and less than that of the blank system [50,51]. Thus, the greater surface roughness is observed for the steel coupon immersed in 0.5 M H_2SO_4, without inhibitor than that of the polished metal coupon. It indicates the mild steel surface becomes rougher in acid medium, without the inhibitor. The roughness probably decreases, due to the protective barrier layer formation on metal surface on the addition of inhibitor and the surface becoming smoother. The parameters derived from the three dimensional AFM morphologies and AFM cross sectional profiles show that the R_q, R_a and R_y values for inhibitors decreases compared to those of blank studies.

This observations prove that the surface is smoother in presence of inhibitor due to the layer formation and also the protective film is in nanometer scale of all the inhibitors *Annona squamosa* in 0.5 M H_2SO_4. It also proves *Annona squamosa* has the maximum inhibition efficiency. The same trend is observed in weight loss as well as polarization and impedance analyses.

Conclusion

Annona squamosa extract can be used as corrosion inhibitor in controlling the corrosion of mild steel immersed in 0.5 M H_2SO_4 solution. The higher concentration of inhibitor is the lower corrosion rate and the higher corrosion inhibition efficiency. Weight loss experiment shows that maximum inhibition efficiency of the high concentration of inhibitor is 97.8%. Electrochemical studies confirmed the formation of a protective film over the mild steel surface. Polarization studies show the extracts of *Annona squamosa* act as cathodic inhibitor, which control the cathodic reaction predominantly. Polarization experiment also shows the similar results to that of weight loss experiment. The surface analysis such as FTIR, UV visible spectra have been carried out to confirm the formation of protective film over the mild steel surface. The SEM and AFM techniques have been used to observe the microstructure of mild steel in the absence and presence of inhibitor. It showed that *Annona squamosa* extract have effectiveness in preventing corrosion of mild steel in 0.5 M H_2SO_4 solution.

ACKNOWLEDGEMENTS

The authors are thankful to the Principal and College Management Committee members of Jamal Mohamed College (Autonomous), Tiruchirappalli, India. The authors are also thankful to the DST-FIST for providing instrumental facilities.

CONFLICT OF INTEREST

The authors declare that there is no conflict of interests regarding the publication of this article.

REFERENCES

1. M. Finšgar and J. Jackson, *Corros. Sci.*, **86**, 17 (2014); https://doi.org/10.1016/j.corsci.2014.04.044
2. I.A. Kartsonakis and C.A. Charitidis, *Appl. Sci.*, **10**, 6594 (2020); https://doi.org/10.3390/app10186594
3. M. Faisal, A. Saeed, D. Shahzad, N. Abbas, F.A. Larik, P.A. Channar, T.A. Fattah, D.M. Khan and S.A. Shehzadi, *Corros. Rev.*, **36**, 507 (2018); https://doi.org/10.1515/corrrev-2018-0006
4. C.I.C. Pinheiro, J.L. Fernandes, L. Domingues, A.J.S. Chambel, I. Graça, N.M.C. Oliveira, H.S. Cerqueira and F.R. Ribeiro, *Ind. Eng. Chem. Res.*, **51**, 1 (2012); https://doi.org/10.1021/ie200743c
5. K. Rose, B.S. Kim, K. Rajagopal, S. Arumugam and K. Devarayan, *J. Mol. Liq.*, **214**, 111 (2016); https://doi.org/10.1016/j.molliq.2015.12.008
6. O. Olawale, B.T. Ogunsemi, J.O. Bello, P.P. Ikubanni, S.J. Ogundipe and T.S. Abayomi, *Int. J. Mech Eng. Technol.*, **9**, 1274 (2018).
7. A. Khadraoui, A. Khelifa, K. Hachama and R. Mehdaoui, *J. Mol. Liq.*, **214**, 293 (2016); https://doi.org/10.1016/j.molliq.2015.12.064
8. N. Gunavathy and S.C. Murugavel, *J. Environ. Nanotechnol.*, **2**, 45 (2013); https://doi.org/10.13074/jent.2013.12.132049
9. A. El Bribri, M. Tabyaoui, B. Tabyaoui, H. El Attari and F. Bentiss, *Mater. Chem. Phys.*, **141**, 240 (2013); https://doi.org/10.1016/j.matchemphys.2013.05.006
10. P. Mourya, S. Banerjee and M.M. Singh, *Corros. Sci.*, **85**, 352 (2014); https://doi.org/10.1016/j.corsci.2014.04.036
11. L. Li, X. Zhang, J. Lei, J. He, S. Zhang and F. Pan, *Corros. Sci.*, **63**, 82 (2012); https://doi.org/10.1016/j.corsci.2012.05.026
12. A. Rajendran, *Int. J. Pharm. Tech. Res.*, **3**, 1005 (2011).
13. O. Olawale, B.T. Ogunsemi, O.O. Agboola, M.B. Ake and G.O. Jawando, *Int. J. Mech. Eng. Technol.*, **9**, 282 (2018).
14. A.Y. El-Etre, *Mater. Chem. Phys.*, **108**, 278 (2008); https://doi.org/10.1016/j.matchemphys.2007.09.037
15. M. Prabakaran, S.H. Kim, K. Kalaiselvi, V. Hemapriya and I.M. Chung, *J. Taiwan Inst. Chem. Eng.*, **59**, 553 (2016); https://doi.org/10.1016/j.jtice.2015.08.023
16. E. Alibakhshi, M. Ramezanzadeh, G. Bahlakeh, B. Ramezanzadeh, M. Mahdavian and M. Motamedi, *J. Mol. Liq.*, **255**, 185 (2018); https://doi.org/10.1016/j.molliq.2018.01.144
17. A. Dehghani, G. Bahlakeh, B. Ramezanzadeh and M. Ramezanzadeh, *Constr. Build. Mater.*, **245**, 118464 (2020); https://doi.org/10.1016/j.conbuildmat.2020.118464
18. M. Keramatinia, B. Ramezanzadeh and M. Mahdavian, *J. Taiwan Inst. Chem. Eng.*, **105**, 134 (2019); https://doi.org/10.1016/j.jtice.2019.10.005
19. M.T. Majd, S. Akbarzadeh, M. Ramezanzadeh, G. Bahlakeh and B. Ramezanzadeh, *J. Mol. Liq.*, **297**, 111862 (2020); https://doi.org/10.1016/j.molliq.2019.111862
20. A. Dehghani, G. Bahlakeh, B. Ramezanzadeh and M. Ramezanzadeh, *J. Mol. Liq.*, **299**, 112220 (2020); https://doi.org/10.1016/j.molliq.2019.112220
21. G. Bahlakeh, A. Dehghani, B. Ramezanzadeh and M. Ramezanzadeh, *J. Mol. Liq.*, **293**, 111559 (2019); https://doi.org/10.1016/j.molliq.2019.111559
22. A. Dehghani, G. Bahlakeh and B. Ramezanzadeh, *Bioelectrochem.*, **130**, 107339 (2019); https://doi.org/10.1016/j.bioelechem.2019.107339
23. R. Anita and M. Chander, *Int. J. Pharmacog. Phytochem.*, **9**, 119 (2017).
24. T.S. Mohamed Saleem and V. Hema Basnett, *Nat. Prod. An Indian J.*, **5**, 85 (2009).
25. K.S. Shanker, S. Kanjilal, B.V. Rao, K.H. Kishore, S. Misra and R.B.N. Prasad, *Phytochem. Anal.*, **18**, 7 (2007); https://doi.org/10.1002/pca.942
26. Z. Begum, I. Younus and S.M. Ali, *World J. Pharm. Pharm. Sci.*, **4**, 116 (2015).
27. S. Gunavathy and S. Murugavel, *E-J. Chem.*, **9**, 487 (2012); https://doi.org/10.1155/2012/952402

28. M.A. El-Hashemy and A. Sallam, *J. Mater. Res. Technol.*, **9**, 13509 (2020); https://doi.org/10.1016/j.jmrt.2020.09.078
29. P. Roy, T. Maji, S. Dey and D. Sukul, *RSC Adv.*, **5**, 61170 (2015); https://doi.org/10.1039/C5RA12266J
30. S. Manimegalai and P. Manjula, *J. Mater. Environ. Sci.*, **6**, 1629 (2015).
31. M. Al-Hashemy and A. Sallam, *J. Mater. Environ. Sci.*, **10**, 840 (2019).
32. A.S. Yaro, R.K. Wael and A.A. Khadom, *J. Univ. Chem. Technol. Metallur*., **45**, 443 (2010).
33. S.S. Syed Abuthahir A.J. Abdul Nasser and S. Rajendran, *Open Mater. Sci. J.*, **8**, 71 (2014); https://doi.org/10.2174/1874088X01408010071
34. V.R. Nazeera Banu, S. Rajendran and S.S. Syed Abuthahir, *Int. J. Chem. Concepts*, **3**, 161 (2017).
35. K.K. Kumar, S.K. Selvaraj, M. Pandeeswaran, S.S. Syed Abuthahir and A. John Amalraj, *Int. J. Adv. Chem. Sci. Appl.*, **3**, 54 (2015).
36. F. Zucchi and I.H. Omar, *Surf. Technol.*, **24**, 391 (1985); https://doi.org/10.1016/0376-4583(85)90057-3
37. M.P. Chakravarthy and K.N. Mohana, *ISRN Corrosion*, **2014**, 687276 (2014); https://doi.org/10.1155/2014/687276
38. R.J. Tuama, M.E. Al-Dokheily and M.N. Khalaf, *Int. J. Corros. Scale Inhib.*, **9**, 427 (2020); https://doi.org/10.17675/2305-6894-2020-9-2-3
39. P.A. Jeeva, G.S. Mali, R. Dinakaran, K. Mohanam and S. Karthikeyan, *Int. J. Corros. Scale Inhib.*, **8**, 1 (2019); https://doi.org/10.17675/2305-6894-2019-8-1-1
40. P. Shanthy, J.A. Thangakani, S. Karthika, S.C. Joycee, S. Rajendran and J. Jeyasundari, *Int. J. Corros. Scale Inhib.*, **10**, 331 (2021); https://doi.org/10.17675/2305-6894-2021-10-1-19
41. M. Barrahi, H. Elhartiti, A. El Mostaphi, N. Chahboun, M. Saadouni, R. Salghi, A. Zarrouk and M. Ouhssine, *Int. J. Corros. Scale Inhib.*, **8**, 937 (2019); https://doi.org/10.17675/2305-6894-2019-8-4-9
42. P. Mahalakshmi, S. Rajendran, G. Nandhini, S.C. Joycee, N. Vijaya, T. Umasankareswari and N. Renuga Devi, *Int. J. Corros. Scale Inhib.*, **9**, 706 (2020); https://doi.org/10.17675/2305-6894-2020-9-2-20
43. W.M.K.W.M. Ikhmal, M.Y.N. Yasmin, M.F.F. Maria1, S.M. Syaizwadi, W.A.W. Rafizah, M.G.M. Sabri and B.M. Zahid, *Int. J. Corros. Scale Inhib.*, **9**, 118 (2020); https://doi.org/10.17675/2305-6894-2020-9-1-7
44. A. Grace Baby, S. Rajendran, V. Johnsirani, A. Al-Hashem, N. Karthiga and P. Nivetha, *Int. J. Corros. Scale Inhib.*, **9**, 979 (2020); https://doi.org/10.17675/2305-6894-2020-9-3-12
45. S. Rajendran, R. Srinivasan, R. Dorothy, T. Umasankareswari and A. Al-Hashem, *Int. J. Corros. Scale Inhib.*, **8**, 437 (2019); https://doi.org/10.17675/2305-6894-2019-8-3-1
46. A. Peter and S.K. Sharma, *Int. J. Corros. Scale Inhib.*, **6**, 112 (2017); https://doi.org/10.17675/2305-6894-2017-6-2-2
47. A. Dehghani, G. Bahlakeh, B. Ramezanzadeh and M. Ramezanzadeh, *Constr. Build. Mater.*, **245**, 118464 (2020); https://doi.org/10.1016/j.conbuildmat.2020.118464
48. N. Kicir, G. Tansug, M. Erbil and T. Tüken, *Corros. Sci.*, **105**, 88 (2016); https://doi.org/10.1016/j.corsci.2016.01.006
49. C. Verma, E.E. Ebenso, I. Bahadur and M.A. Quraishi, *J. Mol. Liq.*, **266**, 577 (2018); https://doi.org/10.1016/j.molliq.2018.06.110
50. Y. Zhu, L. Wang, Y. Behnamian, S. Song, R. Wang, Z. Gao, W. Hu and D.H. Xia, *Corros. Sci.*, **170**, 108685 (2020); https://doi.org/10.1016/j.corsci.2020.108685
51. K. Muthamma, P. Kumari, M. Lavanya and S.A. Rao, *J. Bio. Tribo. Corros.*, **7**, 10 (2021); https://doi.org/10.1007/s40735-020-00439-7